Spreading of Completely Wetting or Partially Wetting Power-Law Fluid on Solid Surface

X. D. Wang,[†] Y. Zhang,[‡] D. J. Lee,*[,§] and X. F. Peng[‡]

Department of Thermal Engineering, School of Mechanical Engineering, University of Science & Technology Beijing, Beijing 100083, China, Lab of Phase Change & Interfacial Transport Phenomena, Department of Thermal Engineering, Tsinghua University, Beijing 100084, China, and Department of Chemical Engineering, National Taiwan University, Taipei 106, Taiwan

Received January 29, 2007. In Final Form: May 25, 2007

This study investigated the drop-spreading dynamics of pseudo-plastic and dilatant fluids. Experimental results indicated that the spreading law for both fluids is related to rheological characteristics or power exponent *n*. For the completely wetting system, the evolution of the wetting radius over time can be expressed by the power law $R = at^m$, where the spreading exponent *m* of the dilatant fluids is >0.1 and the spreading exponent *m* of pseudo-plastic fluids is <0.1. The strength of non-Newtonian effects is positively correlated to the extent of deviation from the theoretical value 0.1 of *m* for Newtonian fluids. For the partially wetting system, the power law on the time dependence of the wetting radius no longer holds; therefore, an exponential power law, $R = R_{eq}(1 - \exp(-at^m/R_{eq}))$, is proposed, where R_{eq} denotes the equilibrium radius of drop and *a* is a coefficient. Comparing experimental data with the exponential power law revealed that both are in good agreement.

1. Introduction

Wetting of solid surfaces with liquids has wide applications in printing, painting, adhesion, lubrication, and spraying, and has attracted considerable research interest.[1−10] The time course of a drop radius (*R*) of a completely wetting fluid on a solid substrate is correlated using a simple power law, $R(t) = at^m$, with $m = 1/10$ or $m = 1/8$ in the capillary spreading or in the gravitational spreading regime, respectively.[11] Many studies of completely wetting Newtonian fluids agree with the above-mentioned theoretical prediction.[2−4,8,10,12−34] Blake,[12] conversely, determined that $m = 1/7$ in the capillary regime based on a molecular kinetics approach.

A simple power-law correlation cannot characterize the time course of a drop radius of a spreading partially wetting Newtonian fluid. De Ruijter et al.[35] developed a three-stage spreading process for water or aqueous solutions of ethanol on alkylsilane-treated glass—initially, $R(t) \approx R_0 + bt$, and intermediately, $R(t) \approx t^{0.1}$—while in the final asymptotic stage with the advancing contact angle almost coincident with the static contact angle, $(R_{eq} - R(t)) \approx \exp(-t/T)$, where R_{eq} is the equilibrium radius and *T* is a characteristic time constant. Barh et al.[36] investigated drop spreading of partially wetting Newtonian fluids (water, and aqueous solutions of ethanol, ethylene glycol, or glycerol on hydrophobic surfaces) and determined that low-viscosity partially wetting fluid rapidly spreads and then abruptly stops in 30 μs, whereas high-viscosity fluid (solutions of ethylene glycol and glycerol) spread over a long period of time following $R(t) \approx t^{1/10}$.

Numerous polymer solutions and solid suspensions show non-Newtonian characteristics. Some theoretical and experimental studies investigated how non-Newtonian fluids spread over solid substrates.[37−41] However, to date only Rafai and Bonn[42,43]

[†] University of Science & Technology Beijing.
[‡] Tsinghua University.
[§] National Taiwan University.

(1) Dussan, V. E. B. *Annu. Rev. Fluid Mech.* **1979**, *11*, 371.
(2) Marmur, A. *Adv. Colloid Interface Sci.* **1983**, *19*, 75.
(3) de Gennes, P. G. *Rev. Mod. Phys.* **1985**, *57*, 827.
(4) Cazabat, A. M. *Contemp. Phys.* **1987**, *28*, 347.
(5) Leger, L.; Joanny, J. F. *Rep. Prog. Phys.* **1992**, *55*, 431.
(6) de Coninck, J.; de Ruijter, M. J.; Voue, M. *Curr. Opin. Colloid Interface Sci.* **2001**, *6*, 49.
(7) Starov, V. M. *Adv. Colloid Interface Sci.* **1992**, *39*, 147.
(8) Lopez, J.; Miller, C. A.; Ruckenstein, E. *J. Colloid Interface Sci.* **1976**, *53*, 460.
(9) Starov, V. M.; Kalinin, V. V.; Chen, J. D. *Adv. Colloid Interface Sci.* **1994**, *50*, 187.
(10) Teletzke, G. F.; Davis, T. H.; Scriven, L. E. *Chem. Eng. Commun.* **1987**, *55*, 41.
(11) Tanner, L. H. *J. Phys. D* **1979**, *12*, 1473.
(12) Blake, T. D.; Haynes, J. M. *J. Colloid Interface Sci.* **1969**, *30*, 421.
(13) Reznik, S. N.; Yarin, A. L. *Phys. Fluids* **2002**, *14*, 118.
(14) Ehrhard, A.; Davis, S. H. *J. Fluid Mech.* **1991**, *229*, 365.
(15) Seaver, A. E.; Berg, J. C. *J. Appl. Polym. Sci.* **1994**, *52*, 431.
(16) Lin, C. M.; Ybarra, R. M.; Neogi, P. *Adv. Colloid Interface Sci.* **1996**, *67*, 185.
(17) Gu, Y.; Li, D. *Colloids Surf., A* **1998**, *142*, 243.
(18) Rieutord, F.; Rayssac, O.; Moriceau, H. *Phys. Rev. E.* **2000**, *62*, 6861.
(19) Voinov, O. V. *J. Colloid Interface Sci.* **2000**, *226*, 22.
(20) Chen, E. C.; Overall, J. C. K.; Phillips, C. R. *Can. J. Chem. Eng.* **1974**, *52*, 71.
(21) Levinson, P.; Cazabat, A. M.; Cohen-Stuart, M. A.; Heslot, F.; Nicolet, S. *Rev. Phys. Appl.* **1988**, *23*, 1009.
(22) Ehrhard, P. *J. Fluid Mech.* **1993**, *257*, 463.
(23) van Oene, H.; Chang, Y. F.; Newman, S. *J. Adhes.* **1969**, *1*, 54.
(24) Lau, W. W. Y.; Burns, C. M. *J. Colloid Interface Sci.* **1973**, *45*, 295.
(25) Ogarev, V. A.; Timonina, T. N.; Arslanov, V. V.; Trapezniko, A. A. *J. Adhes.* **1974**, *6*, 337.
(26) Hyypia, J. *Anal. Chem.* **1948**, *20*, 1039.
(27) Schonhorn, H.; Frisch, H. L.; Kwei, T. K. *J. Appl. Phys.* **1966**, *37*, 4967.
(28) Radigan, W.; Ghirardella, H.; Frisch, H. L.; Schonhorn, H.; Kwei, T. K. *J. Colloid Interface Sci.* **1974**, *49*, 241.
(29) Chen, J. D. *J. Colloid Interface Sci.* **1988**, *122*, 60.
(30) Foister, R. T. *J. Colloid Interface Sci.* **1990**, *136*, 266.
(31) Chen, J. D.; Wada, N. *J. Colloid Interface Sci.* **1992**, *148*, 207.
(32) Ausserre, D.; Picard, A. M.; Leger, L. *Phys. Rev. Lett.* **1986**, *57*, 2671.
(33) Cazabat, A. M.; Cohen-Stuart, M. A. *J. Phys. Chem.* **1986**, *90*, 5845.
(34) Redon, C.; Brochard-Wyart, F.; Hervet, H.; Rondelez, F. *J. Colloid Interface Sci.* **1992**, *149*, 580.
(35) de Ruijter, M. J.; de Coninck Oshanin, G. *Langmuir* **1999**, *15*, 2209.
(36) von Bahr, M.; Tiberg, F.; Yaminsky, V. *Colloids Surf., A* **2001**, *193*, 85.
(37) Pearson, J. R. A. *Mechanics of Polymer Processing*; Elsevier: London, 1985.
(38) Carré, A.; Eustache, F. *Langmuir* **2000**, *16*, 2936.
(39) Starov, V. M.; Tyatyushkin, A. N.; Velarde, M. G.; Zhdanov, S. A. *J. Colloid Interface Sci.* **2003**, *257*, 284.
(40) Betelu, S. I.; Fontelos, M. A. *Appl. Math. Lett.* **2003**, *16*, 1315.
(41) Betelu, S. I.; Fontelos, M. A. *Math. Comput. Model* **2004**, *40*, 729.
(42) Rafai, S.; Bonn, D.; Boudaoud, A. *J. Fluid Mech.* **2004**, *513*, 77.
(43) Rafai, S.; Bonn, D. *Physica A* **2005**, *358*, 58.

10.1021/la700232y CCC: $37.00
Published on Web 08/03/2007

Table 1. Characteristics of Fluids Tested

liquid	type	σ (mN/m)	μ(Pa s) or k (Pa s^n)	n	θ_0 (°)	solid
silicone oil	Newtonian	21.04	1.500	1	0	glass slide
PPG	Newtonian	32.37	0.1158	1	0	glass slide
PPG+7.5% w/w 10 nm silica	dilatant	32.54	0.0711	1.303	0	glass slide
PPG+10% w/w 10 nm silica	dilatant	32.67	0.0861	1.699	0	glass slide
PPG+17.4% w/w 10 nm silica	dilatant	33.44	0.0970	1.763	9.4	glass slide
PPG+7.5% w/w 15 nm silica	dilatant	36.90	0.0478	1.286	24.4	glass slide
PPG+10% w/w 15 nm silica	dilatant	46.99	0.0705	1.728	26.2	glass slide
1% w/w CMC	pseudo-plastic	39.02	7.234	0.5088	20.2	glass slide
0.05% w/w xanthan	pseudo-plastic	65.93	0.03296	0.6292	20.4/0	glass slide/mica
0.1% w/w xanthan	pseudo-plastic	54.62	0.08872	0.5088	24.6/0	glass slide/mica
0.2% w/w xanthan	pseudo-plastic	48.41	0.2847	0.4378	26.5/0	glass slide/mica
0.5% w/w xanthan	pseudo-plastic	49.90	3.529	0.2260	34.4/0	glass slide/mica
1.0% w/w xanthan	pseudo-plastic	43.55	7.990	0.1930	34.5/0	glass slide/mica

experimentally determined the radii of spreading drops of two non-Newtonian fluids, a xanthan solution and a polyacrylamide solution, on a mica surface. Both fluids are completely wetting fluids with a spreading exponent of $<1/10$. Although with some deviation, Rafai and Bonn's results correlated with the theoretical model proposed by Starov et al.[39]

No experimental data exists for spreading radii of partially wetting power-law fluids. Moreover, no further experimental confirmation on the model of Starov et al.[9] is available using completely wetting fluids. This work experimentally determines the time courses of radii of spreading drops for completely and partially wetting power-law fluids, whose shear stress (τ) depending on shear rate (γ) can be expressed as follows:

$$\tau = k\dot{\gamma}^n \tag{1}$$

where k denotes the consistency coefficient, and n represents the power exponent. Correlations applied to both pseudo-plastic ($n < 1$) and dilatant ($n > 1$) fluids were investigated.

2. Experimental Section

2.1. Samples. All chemicals were of highest purity and obtained from Sigma-Aldrich (Taiwan). All chemicals were used without further purification.

Clean microscopic glass slides and mica were the solid substrates tested. All experiments were conducted using the same glass slide, which was cleaned using detergent, ultrapure water, 99.5% ethanol, 2 N nitric acid, and acetone via ultrasonication. Mica foils were split carefully to acquire clean and smooth surfaces. Prior to each experiment, dry nitrogen was utilized to dry the slide or mica.

Silicon oil (surface tension, 21.04 mN m^{-1}; viscosity, 1.5 Pa s) and poly(propylene glycol) (PPG) solution (surface tension, 32.37 mN m^{-1}; viscosity, 0.1158 Pa s) were the test Newtonian fluids. The following five dilatant fluids were used: PPG+7.5% w/w 10 nm silica powders; PPG+10% w/w 10 nm silica; PPG+17.4% w/w 10 nm silica; PPG+7.5% w/w 15 nm silica; and PPG+10% w/w 15 nm silica. The following six pseudo-plastic fluids were tested: 1 wt % carboxymethylcellulose (CMC, sodium salt; MW 700 000 Da) aqueous solution; and 0.05−1% w/w of xanthan solutions.

2.2. Measurements and Tests. Surface tensions of all tested liquids were measured using a Krúss Processor Tensiometer K12 (Krúss GmbH, Hamburg, Germany). A cone-plate rheometer (Advanced Rheometric Expansion System) measured the viscosity vs shear rate relationship for all test liquids.

The static contact angle and drop spreading dynamics tests were performed using an FTA125 Dynamic Contact Angle Analyzer (Contact Angle and Surface Tension Instruments, Portsmouth, USA). A drop of selected liquid (4 μL) was deposited from the top of the horizontally placed substrate.

Images of deposited drops, which were recorded at 60 frames s^{-1} using a CCD camera, were sent to a computer for storage and processing. The contact angle $\theta(t)$ and the wetting radius $R(t)$ as function of time t were acquired by analyzing each frame with built-in software using nonspherical fitting. The static contact angle was determined at the end of each spreading test. At least four identical tests were performed under each experimental condition to ensure data reproducibility.

Table 2. Best-Fit Spreading Exponents and Power Exponents for Eq 2

liquid	solid	exponent factor n	spreading exponent m	correlation coefficients R^2
silicone oil	glass slide	1	0.1075	0.9984
PPG	glass slide	1	0.1018	0.9947
PPG+7.5% w/w 10 nm silica	glass slide	1.303	0.1100	0.9987
PPG+10% w/w 10 nm silica	glass slide	1.699	0.1157	0.9948
0.05% w/w xanthan	mica	0.6292	0.07325	0.9799
0.1% w/w xanthan	mica	0.5088	0.06221	0.9942
0.2% w/w xanthan	mica	0.4378	0.04851	0.9757
0.5% w/w xanthan	mica	0.2260	0.04171	0.9815

3. Results

3.1. Suspension Characteristics and Tests. Figure 1 presents the viscosity vs shear rate relationships for all tested liquids. The PPG + silica solutions exhibit shear-thickening behaviors, whereas the CMC and xanthan solutions have shear-thinning behaviors. The consistency coefficient and power exponent in the power-law model were acquired by regressing rheological data for each fluid (Table 1). Table 1 also lists the measured surface tensions and static contact angles for each fluid−solid substrate combination. The PPG+7.5% w/w 10 nm silica powders and PPG+10% w/w 10 nm silica on glass slide were dilatant completely wetting fluids. The PPG+17.4% w/w 10 nm silica, PPG+7.5% w/w 15 nm silica, or PPG+10% w/w 15 nm silica on the glass slide were dilatant partially wetting fluids. The five xanthan solutions were pseudo-plastic completely wetting fluids on the mica surface, whereas all six pseudo-plastic fluids tested were pseudo-plastic partially wetting fluids on the glass slide.

A spreading test for silicone oil on the glass slide was utilized to verify the reliability of the test apparatus. Silicon oil completely wetted the glass slide; the drop radius followed Tanner's law ($R \approx t^{1/10}$) (Figure 2a) and the dynamic contact angle (θ_D) followed the Hoffman−Voinov−Tanner law ($\theta_D^3 = c_T$Ca (Figure 2b), where c_T is a proportional coefficient, and Ca $= (\mu U)/\sigma$ is the capillary number). Since the relative deviation between experimental and theoretical predictions was only 0.33% for spreading dynamics of silicone oil (Figure 2a,b), the data quality of the present experimental apparatus was assumed justified.

3.2. Wetting Dynamics of Completely Wetting Fluids. Figure 3 presents the radii of spreading drops of tested completely wetting

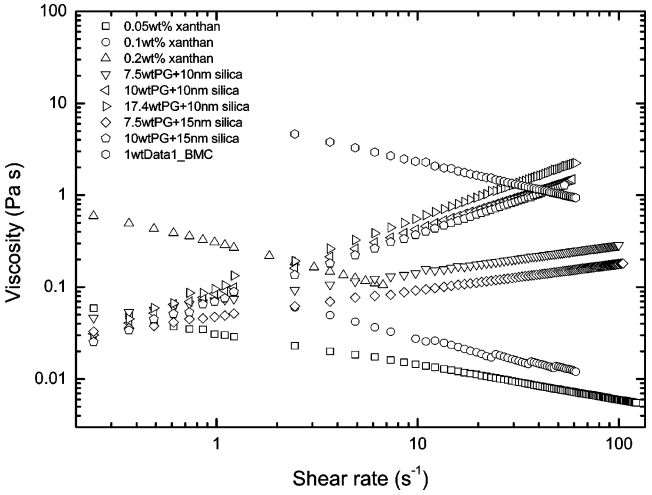

Figure 1. Viscosity vs shear rate of the power-law fluids tested herein.

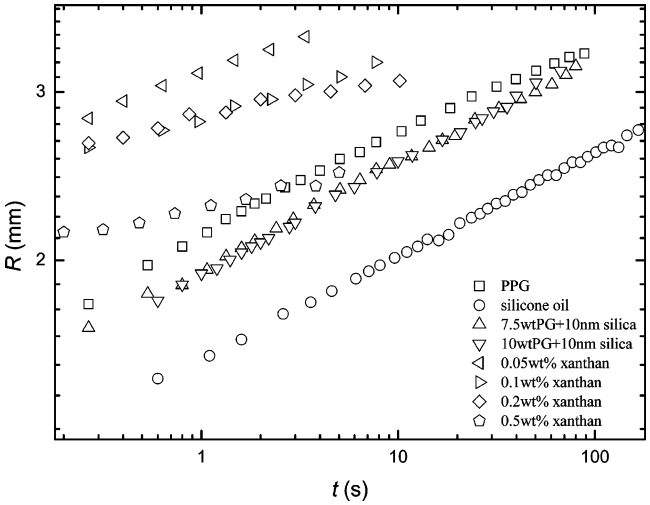

Figure 3. Wetting radius vs spreading time plot of completely wetting fluids.

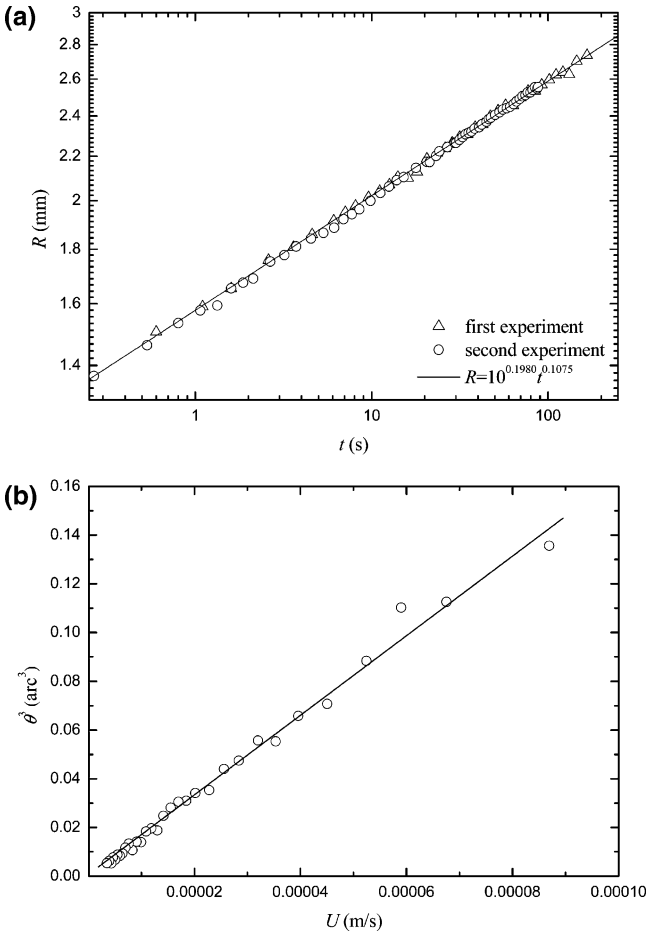

Figure 2. (a) Wetting radius of silicone oil drop on glass slide. Line: Fitting result. (b) Dynamic contact angle of silicone oil drop on glass slide. Line: the Hoffman−Voinov−Tanner law.

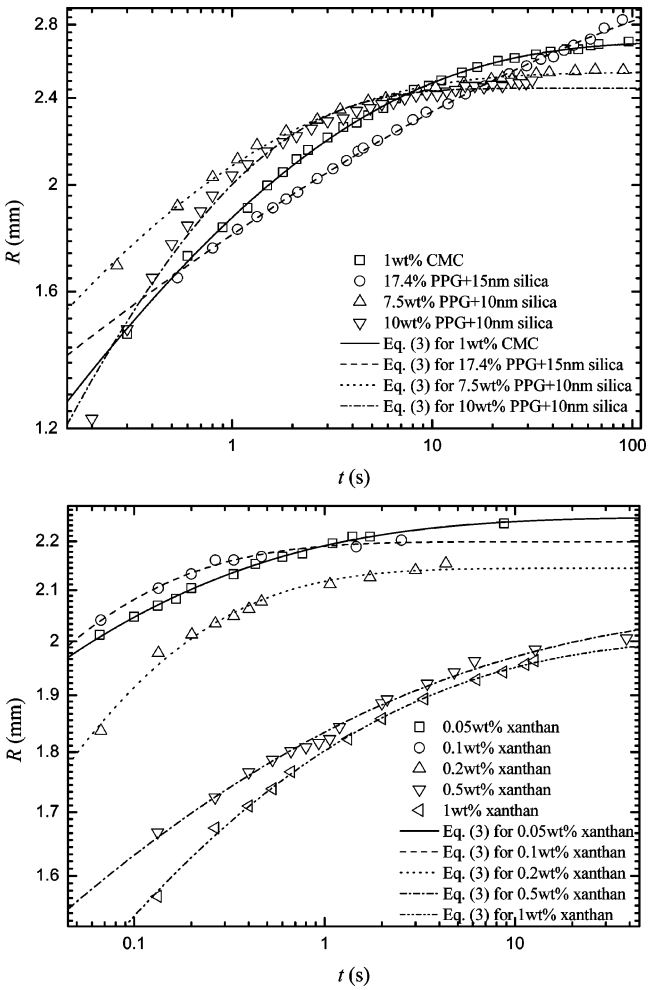

Figure 4. Measured wetting radius of partial wetting power law fluids vs time.

fluids (two Newtonian and six non-Newtonian fluids). With the same drop volume (4 μL), xanthan solution reached a larger spreading radius than PPG suspensions, indicating that xanthan solution had a relatively faster initial spreading. The silicon oil spreads slowly due to its high liquid viscosity.

In the latter stage of spreading, the drop radius vs spreading time exhibited a linear dependence on a log−log scale, implying that the completely wetting fluids, Newtonian and power-law fluids, follow a simple power-law correlation

$$R = at^m \tag{2}$$

Table 2 shows the spreading exponent m and correlation coefficient r^2 acquired for the completely wetting fluids.

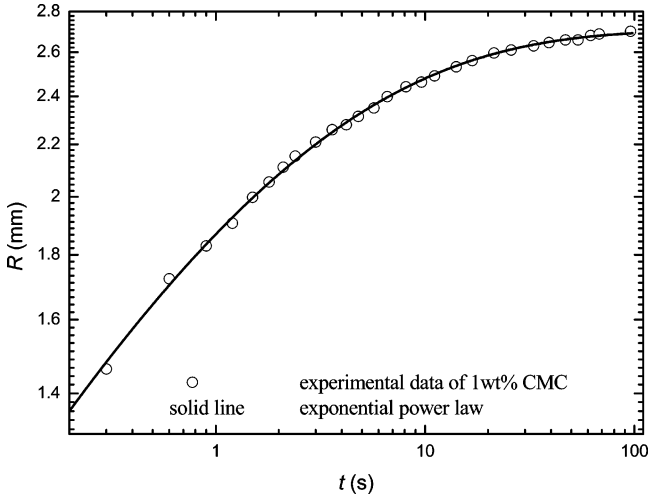

Figure 5. Comparison of wetting radius of 1 wt % CMC and exponential power law.

The spreading exponents for silicone oil and PPG solution were 0.1075 and 0.1018, respectively, close to the theoretical value of 0.1. For pseudo-plastic fluids with $n < 1$, all spreading exponents were <0.1, suggesting that they spread more slowly than their Newtonian counterparts. The spreading exponent (m) declined as the power exponent (n) decreased. The spreading exponents of dilatant fluids were >0.1, suggesting that these fluids spread more rapidly than their Newtonian counterparts.

3.3. Wetting Dynamics of Partially Wetting Fluids. Figure 4 presents the radii of spreading drops of the partially wetting fluids (nine non-Newtonian fluids). The R vs t data did not exhibit a linear dependence on log−log scale as did the completely wetting systems (Figure 3). Moreover, the wetting dynamics of xanthan solutions differed from the CMC solution and PPG + silica suspensions.

For partially wetting Newtonian fluids, de Ruijter et al.[35] divided the spreading process into three stages: initial, $R(t) \approx R_0 + at$; an the intermediate stage; and finally, $R(t) \approx t^{0.1}$. These two asymptotes were noticeable in each test in Figure 4, with the 1% w/w CMC test (Figure 6) as an example. To cover the entire wetting range, we proposed an empirical correlation with a radius scaled by the equilibrium radius as follows:

$$R = R_{eq}\left[1 - \exp\left(-\frac{a}{R_{eq}}t^m\right)\right] \quad (3)$$

For the completely wetting system, $R_{eq} \rightarrow \infty$, so eq 3 becomes $R = at^m$, the correlation for completely wetting systems (eq 2). The higher m corresponds to fast drop spreading on a substrate.

Parameters a and m were utilized as fitting parameters for linearly regressing $R(t)$ with a known R_{eq}. Equation 3 was rearranged into the following linear form:

$$\ln\left[-R_{eq}\ln\left(1 - \frac{R}{R_{eq}}\right)\right] = \ln a + m \ln t \quad (4)$$

Table 3 lists the fitting parameters. Figure 5 compares experimental data for 1% w/w CMC solution and eq 3 with the corresponding best-fit parameters. The agreement between experimental data and correlation was satisfactory.

4. Discussion

By using lubrication theory and similarity transformation, Starov et al.[39] proposed that $R(t) \approx t^{n/3n+5}$ in a gravitational spreading regime, whereas $R(t) \approx t^{n/3n+7}$ in the capillary spreading regime. Figure 6 presents the comparison of the best-fit spreading exponent m in eq 2 using the model developed by Starov et al.[39] The data obtained by Rafai and Boon[42,43] are also shown for comparison (Figure 6).

The capillary length is defined as $k^{-1} = (\sigma/\rho g)^{0.5}$. In the fluids studied, the capillary length was 1.7−2.1 mm for dilatant fluids (PPG suspensions) and 2.2−2.6 mm for pseudo-plastic fluids (CMC and xanthan solutions). Therefore, the drop radius range tested (1.5−3 mm) was in the capillary−gravitational transition regime. The m values for completely wetting dilatant fluids were lower than model predictions for the capillary spreading regime, whereas those for the completely wetting pseudo-plastic fluids were close to those predicted by the capillary spreading regime.

Although eq 3 with a corresponding best-fit parametric set satisfactorily describes the wetting radius vs time data for individual partially wetting power-law fluid, no simple universal correlation existed among the obtained parameters a, m, n, and θ_0 for all fluids tested. The theoretical model predicting spreading dynamics for power-law partially wetting fluids is still lacking.

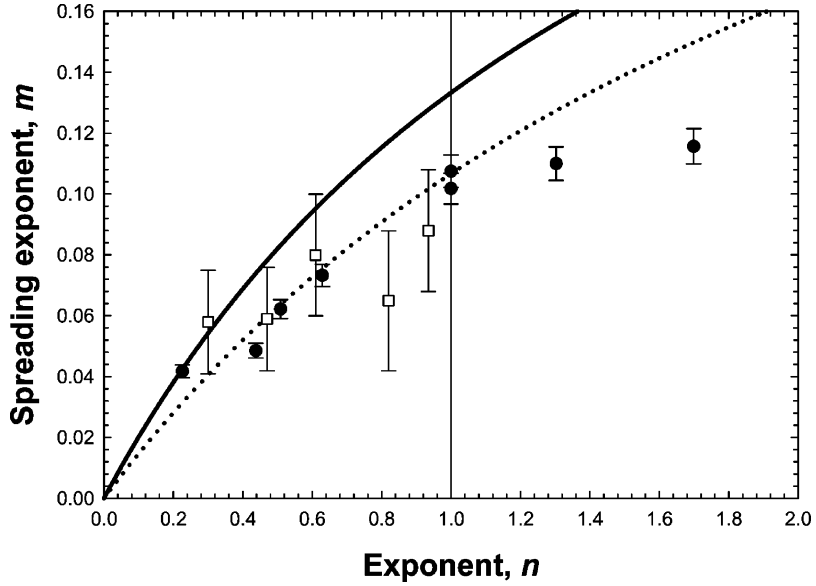

Figure 6. Comparison of spreading exponents of complete wetting fluids with Starov's model. Solid curve: gravitational spreading curve. Dotted curve: capillary spreading curve. Solid circles: present test. Squares: data of Rafai and Boon.[42,43]

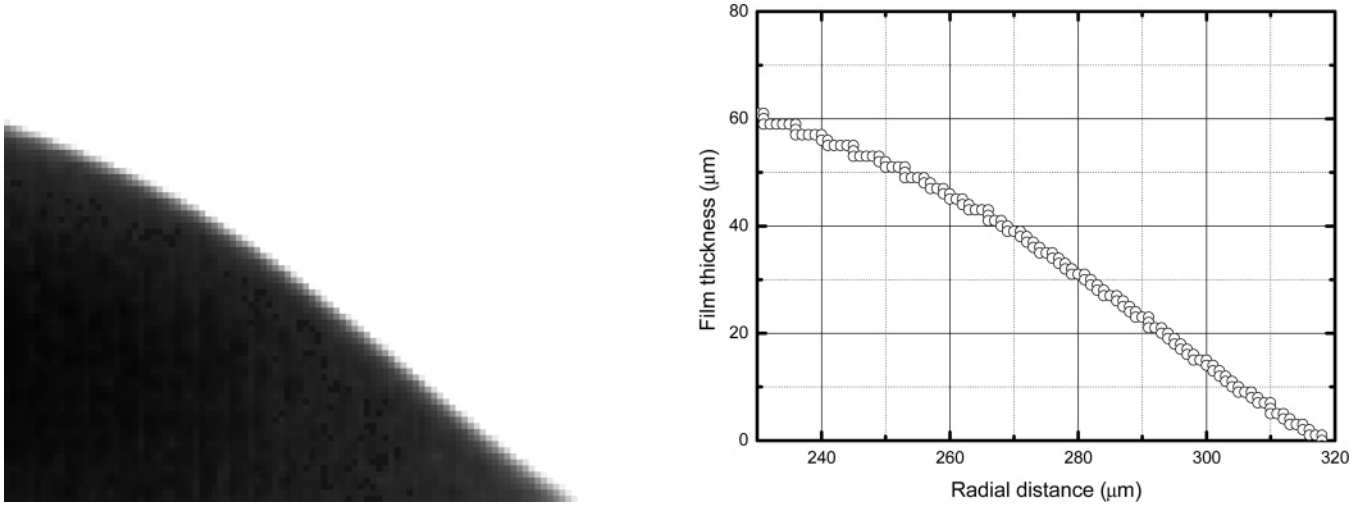

Figure 7. Film profiles near contact line. 0.2 s. 0.5% xanthan solution.

Table 3. Best-Fit Parameters for Partially Wetting, Power-Law Fluids, and Power Exponents for Eq 3

liquid	R_{eq} (m)	a	m	n	θ_0 (°)	correlation coefficient, r^2
1% w/w CMC	0.002702	0.003158	0.3325	0.5088	20.2	0.9991
PPG 17.4% w/w + 10 nm silica	0.003374	0.002577	0.1876	1.763	9.4	0.9989
PPG 7.5% w/w + 15 nm silica	0.002546	0.004317	0.2970	1.303	24.4	0.9970
PPG 10% w/w + 15 nm silica	0.002492	0.003901	0.3820	1.699	26.2	0.9898
0.05% w/w xanthan	0.002238	0.008700	0.2021	0.6292	20.4	0.9984
0.1% w/w xanthan	0.002202	0.01081	0.2174	0.5088	24.6	0.9898
0.2% w/w xanthan	0.002154	0.008401	0.2381	0.4378	26.5	0.9881
0.5% w/w xanthan	0.002006	0.004503	0.1437	0.2260	34.4	0.9916
1.0% w/w xanthan	0.001964	0.004650	0.2040	0.1930	34.5	0.9984

The films near the contact line for the dilatant fluid, Newtonian fluid, and pseudo-plastic fluids differ in shape, as observed by Carre and Eustache.[38] That is, the surface tends to be concave upward for pseudo-plastic fluids (Figure 7) and concave downward for dilatant fluids (image not shown). Image processing identified the location of liquid film for 0.5% w/w xanthan solution spreading on the mica surface at $t = 0.2$ s, yielding the best-fit shape equation of $h \approx x^{1.35}$. With 1% w/w xanthan solution, the corresponding correlation is $h \approx x^{1.40}$. The noted exponents correlated with the predictions by Carre and Eustache.[38]

Acknowledgment. This study was supported by the National Natural Science Foundation of China (no. 50636020).

LA700232Y